



Národní konference s mezinárodní účastí  
**INŽENÝRSKÁ MECHANIKA 2002**

13. – 16. 5. 2002, Svratka, Česká republika

## EVALUATION OF EFFECTIVE PROPERTIES OF WOVEN COMPOSITE TUBES

M. Wierer\*, J. Šejnoha<sup>†</sup>, M. Šejnoha<sup>‡</sup>

**Summary:** *The stepping stone in evaluating effective elastic properties of woven composite tubes is an accurate geometrical description of the composite tube on meso-scale taking the real geometry of the fiber-tow into account. The relevant geometrical parameters obtained from images of real microstructure are provided by a powerful image analyzer Lucie. Furthermore, the periodic character of a fiber-tows arrangement, typical for woven composites, reduces the basic geometrical model to a certain periodic unit cell. Two specific unit cells linked to two different homogenization approaches are introduced. When subjected to suitable periodic boundary conditions, the homogenized unit cells can be periodically extended to map the effective elastic properties over the macroscopic domain under consideration.*

**Keywords:** *Woven composite, micrograph, periodic unit cell, homogenization*

### Introduction

At present, composite materials are still more often used in civil engineering mainly in rehabilitation and repair of concrete and masonry structures. Undoubtable benefits offered by composite materials such as non corrosive properties, light weight, high strength and, of course, design possibilities in shape, structures and colors are the main reason for this boom. Increasing desire for reliable and low cost material systems results in new inexpensive fabrication methods for even larger parts, which can be used in many other applications such as bridge structures, facades and structural parts of commercial and industrial buildings, etc. A polymer matrix system reinforced by glass or graphite

---

\*Mgr. M. Wierer, CTU Faculty of Civil Engineering, Tákturova 7, 166 29 Prague 6

<sup>†</sup>Prof. Ing. J. Šejnoha, DrSc., CTU Faculty of Civil Engineering, Tákturova 7, 166 29 Prague 6, phone +420 2 2435 4492, e-mail: sejnoha@fsv.cvut.cz

<sup>‡</sup>Ing. M. Šejnoha, Ph.D., CTU Faculty of Civil Engineering, Tákturova 7, 166 29 Prague 6, phone +420 2 2435 4494, e-mail: sejnom@fsv.cvut.cz

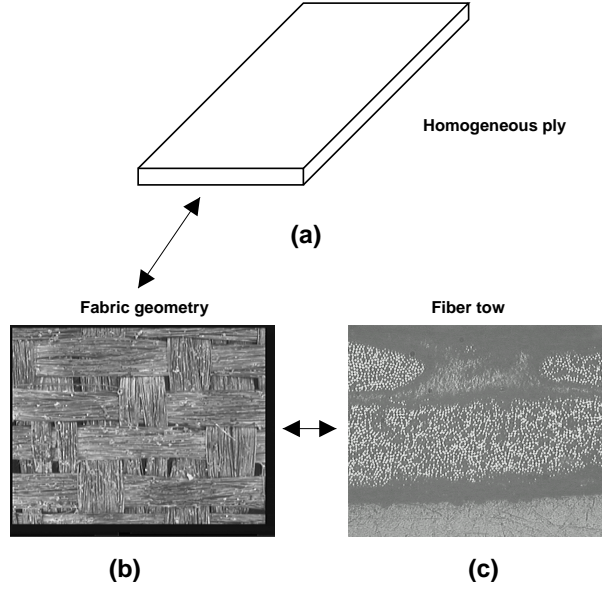


Figure 1: Graphite fiber fabric-polymer matrix composite

fibers appears to be one of the most popular composite material systems. It has been recognized for several years that overall response of such a composite is highly influenced by micromechanical behavior of composite systems.

As suggested in [7, 8], multi-scale modeling is a very useful tool to determine the overall material properties of composite materials and structures. The procedure usually starts by determining the effective elastic properties of a medium on a micro-scale level, Fig. 1(c). To that end, probabilistic methods for homogenization [3, 7] are usually applied. Numerical simulations on the micro-scale level combined with carefully selected laboratory measurements should offer homogenized properties for fiber tow-epoxy matrix mixture displayed in Fig. 1(c). Typically, standard homogenization process based on either periodic unit cell models or the Hashin-Shtrikman variational principles is performed at this level [9].

The next step requires homogenization on a meso-scale level using the geometry of bundles embedded in a matrix, Fig. 1(b). A periodic character of woven composites suggests to formulate a representative volume element in terms of a certain periodic unit cell. Two geometric variants of the periodic unit cell to model interactions between individual phases are presented in Section 1. Each model is linked with a specific homogenization technique. The first approach assumes the original geometric model to be discretized into  $N_1 \times N_2 \times N_3$  pixels. Each pixel represents a center of a cubic element with certain homogenized properties. An iterative numerical method based on Fast Fourier Transforms [5] is then used to evaluate the effective properties of the periodic unit cell. This approach is outlined in Section 3. The second approach, discussed in Section 2, employs the finite element method to solve the relevant boundary value problem. The computational model relies on interconnecting bundles by the polymer matrix contact elements.

Having the effective properties on the meso-scale the procedure concludes with the macroscopic analysis of a large composite structural part, Fig. 1(a).

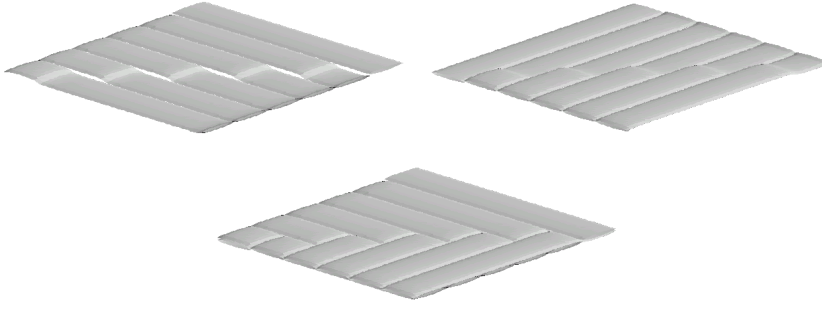


Figure 2: Weave lay-up

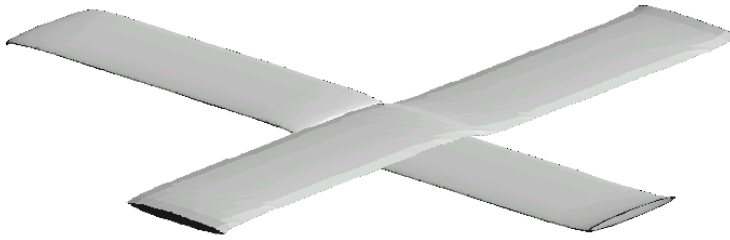


Figure 3: Crossing of bundles

## 1 Geometrical model on meso-scale

For modeling purposes we limit our attention to a two-ply composite tube. Depending on winding speed and orientation the number of bundles within periodically repeating regions may vary. In our particular case, the meso-scale unit cell consists of two plies where each ply contains six bundles. The bundle is formed by unidirectional graphite fibers (approximately 12000 fibers within a bundle) bonded to the polymer matrix. Overall properties of this mixture are found from homogenization procedure carried out on the micro-scale [9]. All six bundles are aligned along the same direction, but they run through individual plies thus creating a typical woven structure of the composite. This is shown schematically in Fig. 2. Fig. 3 depicts an intersection exchange of two bundles, which propagate from one ply into the other.

The shape of the bundle cross-section is derived from images of real composite structure. One typical section is displayed in Fig. 4(a) showing a portion of the bundle cross-section and together with longitudinal variation of the bundle middle curve. With the help of the image analyzer LUCIE such a micrograph can be transformed into a binary image and further analyze to provide all geometrical parameters to build an idealized geometrical model such as the one shown in Fig. 4(b).

The microscopic images of a real tube suggest that every bundle is impregnated by the polymer matrix, the thickness of which is about 0,03 mm. The interface layer between the two bundles is approximately 0,02 mm thick. The same thickness is considered between the two bundles, which are parallel to each other and lay in the same ply. To simplify the geometrical model it is contemplated that the shape of the bundle cross-section is

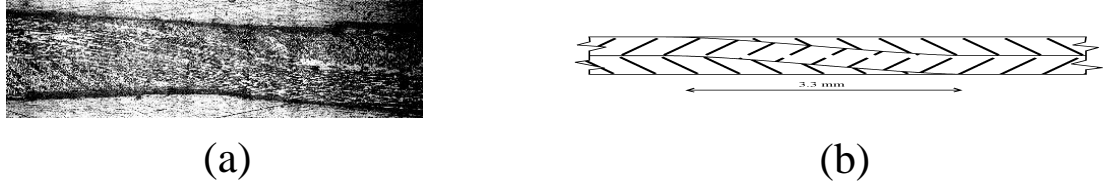


Figure 4: Geometry of fiber bundle

kept constant along the whole bundle. The bundle itself is created by translating the bundle cross-section along the middle-curve, recall Fig. 4(a). A section of the resulting unit cell generated using the above assumptions appears in Fig. 5(a).

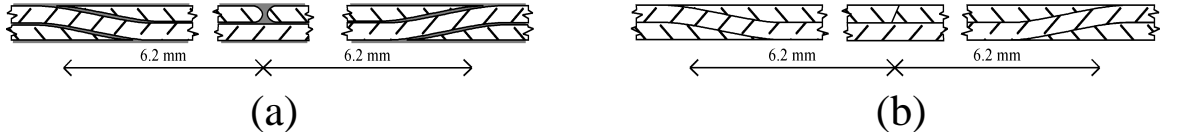


Figure 5: Geometrical model of the unit cell – idealization

Such a geometrical model, however, is not very suitable for computational modeling using the finite element method. The main drawback is a very thin interface layer. Its discretization results in very small elements spread over large region of the unit cell thus leading to enormous computational effort, while not substantially increasing the accuracy of the numerical model. Therefore, in order to arrive at a feasible numerical model, some action must be taken. A suitable method of attack appears in replacing the interface layer by contact elements with zero thickness and appropriate interfacial properties. A section of such a model is depicted in Fig. 5(b). This particular model is used in conjunction with standard homogenization procedure discussed in Section 2. An example of a bundle mesh is shown in Fig. 6 obtained using the automatic mesh generator [6]. On the other hand, a literature offers a powerful homogenization method based on Hashin and Shtrikman [3] idea combined with the Fast Fourier Transform to solve the resulting equations [5], which can be exploited in conjunction with the original unit cell model, Fig. 5(a).

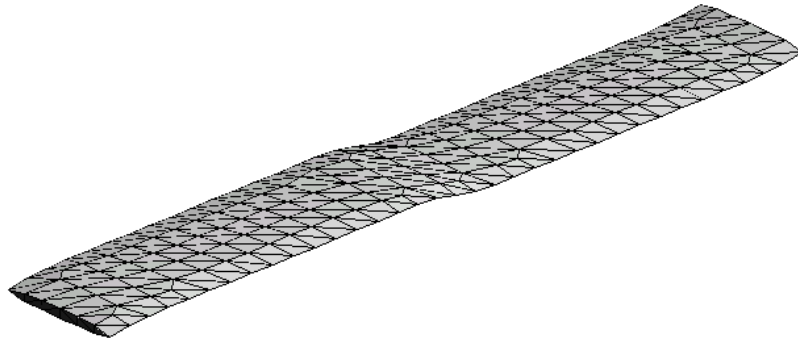


Figure 6: Bundle meshing

## 2 Homogenization based on Finite Element Method

Here we limit our attention to pure mechanical loading and define the following mechanical loading problems

$$\mathbf{u}_0(\mathbf{x}) = \mathbf{E} \cdot \mathbf{x} \quad \mathbf{x} \in S, \quad (1)$$

$$\mathbf{p}_0(\mathbf{x}) = \mathbf{\Sigma} \cdot \mathbf{n}(\mathbf{x}) \quad \mathbf{x} \in S, \quad (2)$$

where  $\mathbf{u}_0$  and  $\mathbf{p}_0$  are the displacement and traction vectors on the external boundary  $S$  of a representative volume element  $\Omega$  of the composite;  $\mathbf{n}$  is the outer unit normal to  $S$ ;  $\mathbf{E}$  and  $\mathbf{\Sigma}$  are the applied macroscopic uniform strain and stress fields, respectively. The macroscopic constitutive relations are then provided by

$$\langle \boldsymbol{\sigma}(\mathbf{x}) \rangle = \langle \mathbf{L}(\mathbf{x}) \boldsymbol{\epsilon}(\mathbf{x}) \rangle = \sum_{r=1}^2 c_r \mathbf{L}_r \langle \boldsymbol{\epsilon}_r(\mathbf{x}) \rangle = \mathbf{L} \mathbf{E} \quad (3)$$

$$\langle \boldsymbol{\epsilon}(\mathbf{x}) \rangle = \langle \mathbf{M}(\mathbf{x}) \boldsymbol{\sigma}(\mathbf{x}) \rangle = \sum_{r=1}^2 c_r \mathbf{M}_r \langle \boldsymbol{\sigma}_r(\mathbf{x}) \rangle = \mathbf{M} \mathbf{\Sigma}, \quad (4)$$

where  $\langle \cdot \rangle$  stands for the spatial average of a given field,  $c_r$  is the volume fraction of the  $r^{th}$  phase, and  $\mathbf{L}$  and  $\mathbf{M}$  are the effective stiffness and compliance matrices of the heterogenous material, respectively. Eqs. (3) and (4) follow directly from Hill's lemma [4]. He proved that for compatible strain and equilibrated stress fields the following relation holds

$$\langle \boldsymbol{\epsilon}(\mathbf{x})^T \boldsymbol{\sigma}(\mathbf{x}) \rangle = \langle \boldsymbol{\epsilon}(\mathbf{x}) \rangle^T \langle \boldsymbol{\sigma}(\mathbf{x}) \rangle, \quad (5)$$

and consequently

$$\mathbf{E}^T \mathbf{L} \mathbf{E} = \langle \boldsymbol{\epsilon}(\mathbf{x})^T \mathbf{L}(\mathbf{x}) \boldsymbol{\epsilon}(\mathbf{x}) \rangle, \quad (6)$$

$$\mathbf{\Sigma}^T \mathbf{M} \mathbf{\Sigma} = \langle \boldsymbol{\sigma}(\mathbf{x})^T \mathbf{M}(\mathbf{x}) \boldsymbol{\sigma}(\mathbf{x}) \rangle. \quad (7)$$

Eq. (5) states in fact that the average of “microscopic” internal work is equal to the macroscopic work done by internal forces. The above relations provide the stepping stone for the derivation of effective properties of composite materials.

Two specific approaches corresponding to loading conditions are mentioned. The first formulation is based on strain approach. We assume that the PUC (a periodic unit cell) is subjected to boundary displacements  $\mathbf{u}_0$  resulting in a uniform strain  $\mathbf{E}$  throughout the body. The second one is based on stress approach. It means that the PUC is loaded by overall stress  $\mathbf{\Sigma}$ . Details can be found in [7].

## 3 Homogenization based on Fast Fourier Transforms

The formulation starts with the definition of a reference medium  $\mathbf{L}_0$ . Then, constitutive equations can be written in the form

$$\boldsymbol{\sigma}(\mathbf{x}) = \mathbf{L}(\mathbf{x}) \boldsymbol{\epsilon}(\mathbf{x}) = \mathbf{L}_0 \boldsymbol{\epsilon}(\mathbf{x}) + \boldsymbol{\tau}(\mathbf{x}), \quad (8)$$

where  $\boldsymbol{\tau}$  is the stress polarization tensor given by

$$\boldsymbol{\tau}(\mathbf{x}) = (\mathbf{L}(\mathbf{x}) - \mathbf{L}_0) \boldsymbol{\epsilon}(\mathbf{x}). \quad (9)$$

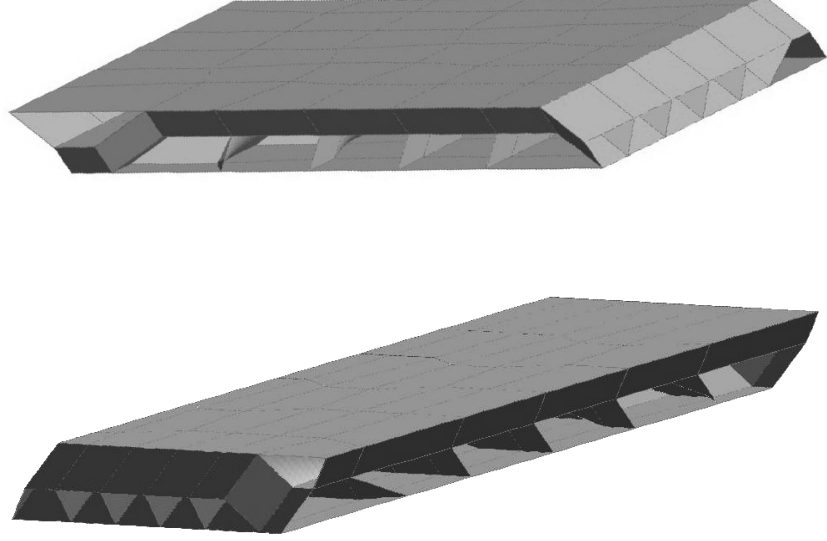


Figure 7: The periodic unit cell for FFT

Once the polarization stress is known, the strain field  $\epsilon(\mathbf{x})$  can be obtained via Green's function  $\Gamma$ , corresponding to a given reference medium

$$\epsilon(\mathbf{x}) = \mathbf{E} - \int_{\Omega} \Gamma(\mathbf{x} - \mathbf{x}') \boldsymbol{\tau}(\mathbf{x}') d\mathbf{x}'. \quad (10)$$

After inserting relation (9) into (10), we obtain the so called *periodic Lippmann-Schwinger* integral equation for a given medium

$$\epsilon(\mathbf{x}) + \int_{\Omega} \Gamma(\mathbf{x} - \mathbf{x}') (\mathbf{L}(\mathbf{x}') - \mathbf{L}_0) \epsilon(\mathbf{x}') d\mathbf{x}' = \mathbf{E}. \quad (11)$$

This equation can be solved by the following iterative procedure:

$$\epsilon^{k+1}(\mathbf{x}) = \mathbf{E} - \int_{\Omega} \Gamma(\mathbf{x} - \mathbf{x}') (\mathbf{L}(\mathbf{x}') - \mathbf{L}_0) \epsilon^k(\mathbf{x}') d\mathbf{x}'. \quad (12)$$

Using the relation

$$\epsilon(\mathbf{x}) = \mathbf{E} + \int_{\Omega} \Gamma(\mathbf{x} - \mathbf{x}') \mathbf{L}_0 \epsilon(\mathbf{x}') d\mathbf{x}' \quad (13)$$

we finally arrive at

$$\epsilon^{k+1}(\mathbf{x}) = \epsilon^k(\mathbf{x}) - \int_{\Omega} \Gamma(\mathbf{x} - \mathbf{x}') \mathbf{L}(\mathbf{x}') \epsilon^k(\mathbf{x}') d\mathbf{x}' \quad (14)$$

$$= \epsilon^k(\mathbf{x}) - \int_{\Omega} \Gamma(\mathbf{x} - \mathbf{x}') \boldsymbol{\sigma}(\mathbf{x}') d\mathbf{x}'. \quad (15)$$

The numerical procedure for solving this equation is based on the fact that the term  $\int_{\Omega} \Gamma(\mathbf{x} - \mathbf{x}') \boldsymbol{\sigma}(\mathbf{x}') d\mathbf{x}'$  can be efficiently evaluated using Fourier transform techniques. To that end, the material is divided into the lattice of  $N_1 \times N_2 \times N_3$  points and appropriate stiffness tensors are assigned to each point. The corresponding stress and strain fields are then obtained by the following process:

0. Initialize:  $k = 0$ ,  $\epsilon^0 = \mathbf{E}$ ,  $\boldsymbol{\sigma}^0 = \mathbf{L}(\mathbf{x})\mathbf{E}$ .

1. Compute  $\widehat{\boldsymbol{\sigma}}^k$  by FFT
2. Convergence test:  $\|\boldsymbol{\xi} \cdot \widehat{\boldsymbol{\sigma}}^k(\boldsymbol{\xi})\| \leq tol$
3. Set

$$\begin{aligned}\widehat{\boldsymbol{\epsilon}}^{k+1}(\boldsymbol{\xi}) &= \widehat{\boldsymbol{\epsilon}}^k - \widehat{\Gamma}(\boldsymbol{\xi})\widehat{\boldsymbol{\sigma}}^k(\boldsymbol{\xi}) \text{ for } \boldsymbol{\xi} \neq \mathbf{0} \\ \widehat{\boldsymbol{\epsilon}}^{k+1}(\boldsymbol{\xi}) &= \mathbf{E} \text{ for } \boldsymbol{\xi} = \mathbf{0}\end{aligned}$$

4. Compute  $\boldsymbol{\epsilon}^{k+1}$  by inverse FFT
5. Set  $\boldsymbol{\sigma}^{k+1}(\mathbf{x}) = \mathbf{L}(\mathbf{x})\boldsymbol{\epsilon}^{k+1}(\mathbf{x})$
6.  $k = k + 1$ , go to 1.

Details regarding this method together with suggestions for the choice of reference material can be found in [5] and references therein.

## 4 Convergence of FFT

The iterative process mentioned above can be expressed in a another way using operator  $\mathbf{I}(\mathbf{L}(\mathbf{x}) - \mathbf{L}_0)$ . The expression (11) is a linear integral equation for  $\boldsymbol{\epsilon}(\mathbf{x})$ . So the solution of the iterative process can be obtained as

$$\boldsymbol{\epsilon}(\mathbf{x}) = \sum_{i=0}^{\infty} (\mathbf{L}(\mathbf{x}) - \mathbf{L}_0)^i \mathbf{E}, \quad (16)$$

where  $(\mathbf{L}(\mathbf{x}) - \mathbf{L}_0)^i$  represents  $i$  consecutive applications of the operator  $(\mathbf{L}(\mathbf{x}) - \mathbf{L}_0)$  to  $\mathbf{E}$ . This so-called Neumann's expansion, is a expression of the inverse of a linear operator of the form  $\mathbf{I} - \mathbf{A}$  as

$$(\mathbf{I} - \mathbf{A})^{-1} = \mathbf{I} + \mathbf{A} + \mathbf{A}^2 + \mathbf{A}^3 + \dots \quad (17)$$

This expansion converges only if  $\|\mathbf{A}\| < 1$ . The convergence of this series for isotropic medium was discused in many papers [12, 5]. For example, if the system consists of several isotropic materials with Lamé's coefficients  $\lambda$  and  $\nu$ , the best choice of the reference medium is an isotropic material with  $\lambda = (\sup \lambda(\mathbf{x}) - \inf \lambda(\mathbf{x}))/2$  and  $\nu = (\sup \nu(\mathbf{x}) - \inf \nu(\mathbf{x}))/2$ . Some other more powerful iterative procedures based on this one were developed. See for example [12].

The problem occurs for anisotropic materials. This problem is not sufficiently explored. Numerical results show, that the choice of the reference medium is a very sensitive process. If the unit cell consists of only isotropic and transversaly isotropic material, the transversaly isotropic material with  $m = \sup m(\mathbf{x})$ ,  $k = \sup k(\mathbf{x})$ ,  $l = \sup l(\mathbf{x})$ ,  $n = \sup n(\mathbf{x})$  and  $p = \sup p(\mathbf{x})$  can be used as the reference medium. The stiffness tensor of transversaly isotropic material is expressed as

$$\mathbf{L}(\mathbf{x}) = \begin{bmatrix} n & l & l & 0 & 0 & 0 \\ l & k+m & k-m & 0 & 0 & 0 \\ l & k-m & k+m & 0 & 0 & 0 \\ 0 & 0 & 0 & m & 0 & 0 \\ 0 & 0 & 0 & 0 & p & 0 \\ 0 & 0 & 0 & 0 & 0 & p \end{bmatrix}. \quad (18)$$

However, when the isotropic material is selected as the reference medium, the convergence of iteration process may fail or slow considerably as it depends on the contrast of material parameters of isotropic and transversely isotropic materials.

The poorest results are gained if the transversely isotropic stiffness tensors are rotated around any axis as  $\mathbf{L}(\mathbf{x}) = \mathbf{Q}^\top(\mathbf{x})\mathbf{L}'(\mathbf{x})\mathbf{Q}(\mathbf{x})$ , where  $\mathbf{Q}(\mathbf{x})$  is the matrix of rotation. The convergence in this case is not reached for any "reasonable" choice of the reference material. Theoretically, the conditions for convergence in this case could be gained with the help of interval matrixes, but we were not able to obtain any reasonable results. For details you can see [10, 11].

## 5 Results obtained by FFT algorithm

In this section results for a 2D example are shown. A unit cell with a hexagonal arrangement of carbon fibers embedded in an epoxy matrix is used. See Fig. 8. This

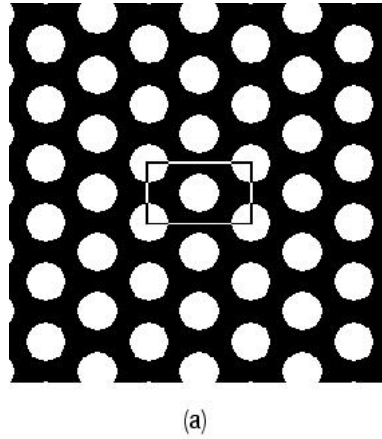


Figure 8: Hexagonal array

unit cell is divided into  $127 \times 73$  pixels and every pixel is assigned material properties (e.g. a stiffness tensor) according to his position. Two isotropic materials, one for carbon fibers and one for the epoxy matrix are used. Three different FFT algorithms are used. 3D algorithm works with the  $6 \times 1$  strain and stress vectors (e.g.  $\epsilon_{11}, \epsilon_{22}, \epsilon_{33}, \epsilon_{12}, \epsilon_{13}, \epsilon_{23}$ ), 2Dgen algorithm uses only inplane components of these fields and a component normal to this plane (e.g.  $\epsilon_{11}, \epsilon_{22}, \epsilon_{12}, \epsilon_{33}$ ) and 2D algorithm, which uses only inplane components (e.g.  $\epsilon_{11}, \epsilon_{22}, \epsilon_{12}$ ). Relation between the speed of convergence and the choice of the reference medium is shown in Fig. 9, where the material properties of the reference medium are defined with the help of  $k$  as:

$$\mu = \mu_{epox} + k(\mu_{carb} - \mu_{epox}) \quad (19)$$

$$\lambda = \lambda_{epox} + k(\lambda_{carb} - \lambda_{epox}), \quad (20)$$

where  $\lambda$  and  $\mu$  mean Lamé's coefficients. The choice of reference medium does not influence the overall material properties of this unit cell. Fig. 10 shows the speed of convergence for  $k = 6$ . The amount of unbalanced stress is used as a convergence criterium. The y-axis is in logarithmic scale. Evidently the speed of convergence is very high, but unfortunately, if we use several different isotropic materials in the unit cell (not



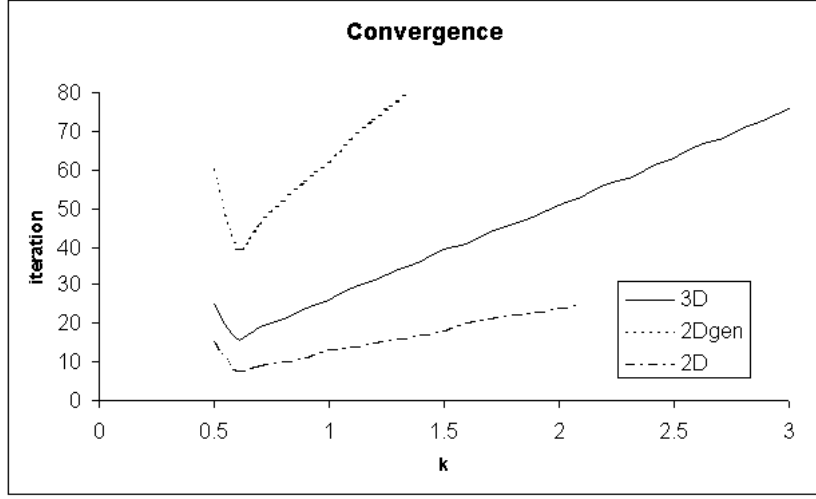


Figure 9: Convergence

only two as in our example), the speed of convergence decreases, but not drastically. Nevertheless, a linear dependence of the convergence speed on the number of isotropic materials is observed.

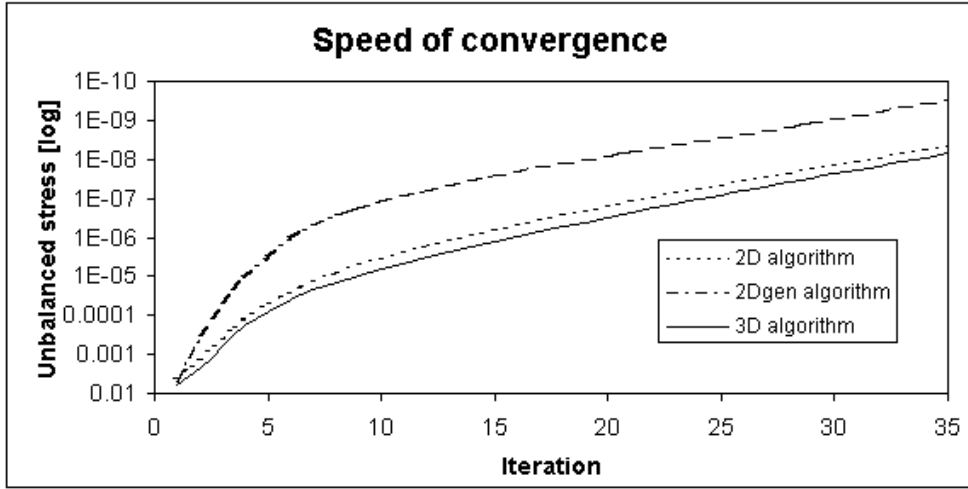


Figure 10: Speed of convergence

## 6 Conclusion

The paper outlines modeling tools applicable to the formulation of meso-scale periodic unit cells. Such unit cells are intended for the evaluation of effective elastic properties of woven composite tubes made of graphite fibers bonded to a polymer matrix. Standard FEM based homogenization procedure and the method based on the Fast Fourier Transform can be implemented to derive the desired results.

## Acknowledgments

Financial support was provided by the GAČR 103/00/0756.

Some of the results published in this paper have been already presented on other conferences.

## References

- [1] Beran, M.J. *Statistical continuum theories*. Intersciens publishers, a division of John Wiley and Sons, New York, (1968).
- [2] Bittnar, Z. and Šejnoha, J. *Numerical methods in structural engineering*. ASCE Press, (1996).
- [3] Drugan, W.J. and Willis, J.R. A micromechanics-based nonlocal constitutive equation and estimates of representative volume element size for elastic composites. *J. Mech. Phys. Sol.*, **44**, 497–524, (1996).
- [3] Hashin, Z. and Shtrikman, S. A variational approach to the theory of the elastic behaviour of multiphase materials. *J. Mech. Phys. Sol.*, **11**, 125–140, (1963).
- [4] Hill, R. Elastic properties of reinforced solids. *J. Mech. Phys. Sol.*, **11**, 357–372, (1963).
- [5] Michel, J.C. and Moulinec, H. and Suquet, P. Effective properties of composite materials with periodic microstructure: A computational approach. *Computer Methods in Applied Mechanics and Engineering*, **172**, 109–143, (1999).
- [6] Rypl, D. *Sequential and Parallel Generation of Unstructured 3D Meshes*. CTU Reports, **3**, 13–91, (1998)
- [7] Šejnoha, M. *Micromechanical analysis of random composites*. Habilitation thesis, Czech Technical University in Prague, (2000).
- [8] Šejnoha, M. and Šejnoha, J. Multiscale Modeling in Engineering. Accepted for publication in *Slovak Journal of Civil Engineering*, (2001).
- [9] Zeman, J. and Šejnoha, M. Numerical evaluation of effective properties of graphite fiber tow impregnated by polymer matrix. *J. Mech. Phys. Sol.*, **49**(1), 69–90, (2001).
- [10] Rohn, J. and Rex, G. Sufficient conditions for regularity and singularity of interval matrices. *SIAM JMAA*, **20**, 437–445, (1996).
- [11] Jansson, J. Calculation of exact bounds for the solution set of linear interval systems. *Lin. Alg. and its Apl.*, **251**, 221–340, (1997).
- [12] Milton, G. W. and Eyre, D. J. A fast numerical computing the response of composites using grid refinement. *EPJ*, (1999).